Growth, Spectral, Computational Studies and Docking Analysis on 2-Aminopyridiniumdibromomethonate Single Crystal

D.Chandrika[a], R.Santhakumari[b]∗

[a-e]Department of Physics, Government Arts College for Women, (Autonomous),
Pudukkottai-622 001 (Affiliated to Bharathidasan university, Tiruchippalli – 620 024),
Tamil Nadu, India
[∗]Corresponding author: santhasrinithi@yahoo.co.in(R.Santhakumari).

Abstract

Slow evaporation was used to create an organic crystal of 2-aminopyridinedibromomomethane (2APDM). Powder X-Ray Diffraction (PXRD) was utilized to validate the crystalline nature and phase purity of the produced crystal, while single crystal X-Ray Diffraction (SXRD) was used to analyse its structural characteristics. The FT-IR spectra of the formed crystal were used to identify different functional groups. UV-Vis-NIR spectroscopy investigations were used to assess the crystal's potential for optical applications. To further investigate the possible intermolecular interactions, Hirshfeld surface analysis was used. The HOMO-LUMO analysis and electronic absorption spectra were determined using density functional theory calculations using B3LYP/6-311++G(d,p) basis sets. The Dipole moment, Polarizability, and Hyperpolarizability, as well as Natural Hyperpolarizability, were calculated using the DFT/B3LYP technique.

Keywords: Crystal growth, Growth from solution, X-ray diffraction, DFT studies, Hirshfeld surface analysis and docking analysis.

1. Introduction

Organic nonlinear optical crystals have a wide range of possible applications, including photonics, frequency doubling, optical switching, modulation, laser remote sensing, and optical device manufacture. Growing crystals with improved nonlinear optical behaviour is also in high demand, with applications in electronics, optical communication, and storage systems [1]. Organic crystals are significant because they serve as a source of light in electro-optics [2-8]. Organic materials' nonlinear behaviour is due to their large degree of delocalized electrons [9]. Organic compounds have significant NLO responses due to the presence of a donor and acceptor network in their molecular structure,

which allows for a wide range of design options.

Organic materials are also advantageous because their synthetic flexibility allows them to adjust optical qualities by improving structural reformation and revealing large later damage thresholds.

New crystals of 2-aminopyridinedibromomethane (2APDM) were developed using a slow evaporation solution growth technique, and XRD, FT-IR, UV-Vis spectroscopy, and theoretical calculations were performed on the grown crystal. The molecule's intermolecular interaction was determined using 3D Hirshfeld surface analysis. The values of the molecules dipole moment (μ), Polarizability(α), and First-order hyperpolarizability(β) were theoretically determined using the DFT analysis. The binding energy, RMSD, and pharmacological activity of the compound were determined by a docking research.

2. Experimental Procedure
2.1 Crystal growth

2-aminopyridine and dibromomethane were equimolorally mixed in water and refluxed for 4 hours. The solution was cooled in a beaker. At the bottom of the beaker, a yellow-colored salt developed. 2APDM produced powder is dissolved in 50 ml water in a beaker and well mixed with a magnetic stirrer. To ensure gradual evaporation, the solution was filtered using microfilter paper

and sealed with a perforated cover. Figure 1 shows the 2APDM single crystals formed after 20 days.

Figure 1.As grown single crystal of 2APDM

3. Result and discussion
3.1. Powder X-ray diffraction (PXRD) studies

Powder XRD patterns for the crystal 2APDM were compared with the simulated SXRD spectral patterns which matches the identities of the grown 2APDM crystals with the data shown in Figure 2. The lattice parameters observed for 2APDM are, a= 5.4965 (5) Å, b= 11.9528 (10) Å, c= 17.7702 (18) Å, β= 95.354 (3) and volume V= 1162.38(19) Å ^{3} with space group P2$_1$/$_C$. The calculated lattice parameter from the PXRD closely matches the reported values [10].
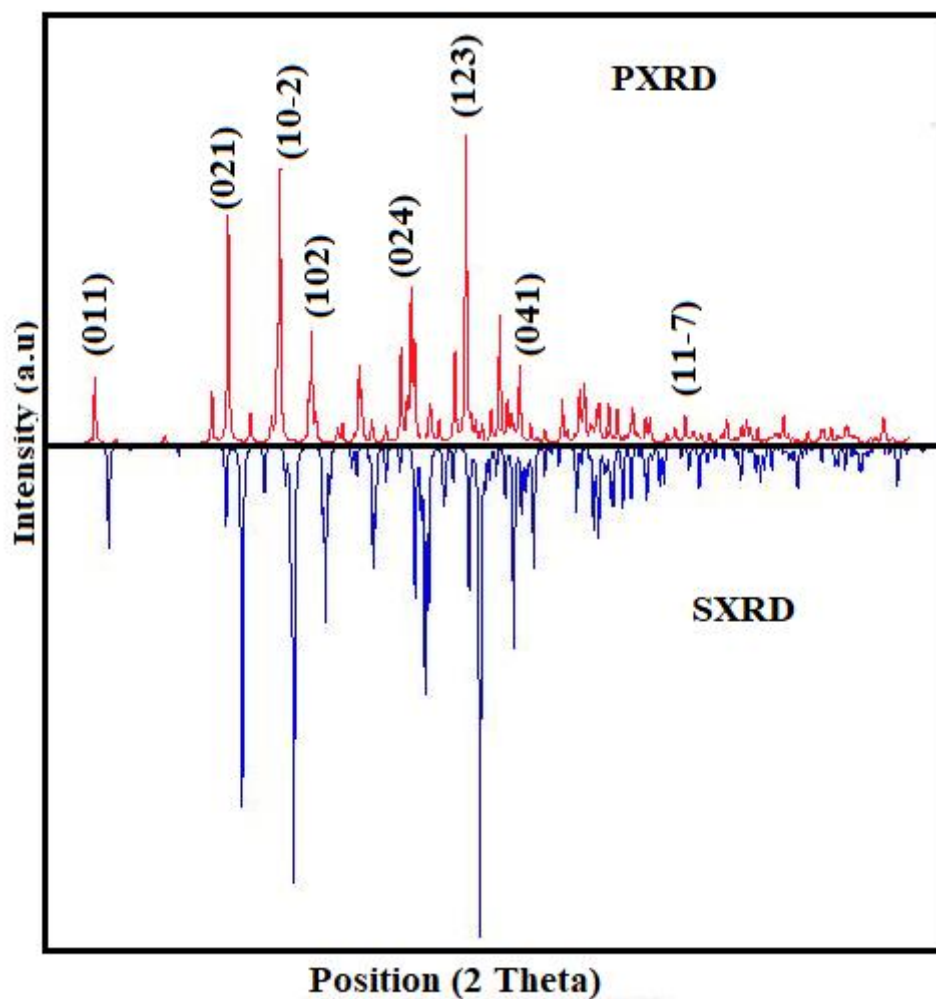
Figure 2.Comparison of SCXRD and PXRD data of 2APDM single crystal

3.2. FT-IR spectral analysis

Figure 3shows the experimental and stimulated FT-IR spectra, respectively. Table 1 shows the spectral vibrations of 2APDM as well as the tentative frequency assignment In the IR and simulated spectra, the CH stretching is found at 2958 cm^{-1}, 2345 cm^{-1} and 2874 cm^{-1}, 2428 cm^{-1}, respectively. The NH asymmetric stretching vibration was observed at 1745 cm^{-1} and 1732 cm^{-1}, in the spectra of IR and DFT, respectively. The FT-IR and DFT counterparts show NO$_2$ asymmetric stretching vibration at 1593 cm^{-1}and 1561 cm^{-1} respectively. The band at

1365 cm^{-1} can be attributed to the CH deformation in IR**.** The vibrational modes at 1219 cm^{-1} and 1187 cm^{-1} correspond to CO stretching in both IR and simulated spectra. The presence of CC stretching vibration is appeared in both spectra by the intense sharp band at 954 cm^{-1} and 913 cm^{-1}. The CBr stretching vibration was observed at 665 cm^{-1} and 630 cm^{-1}, in the spectra of IR and DFT, respectively.
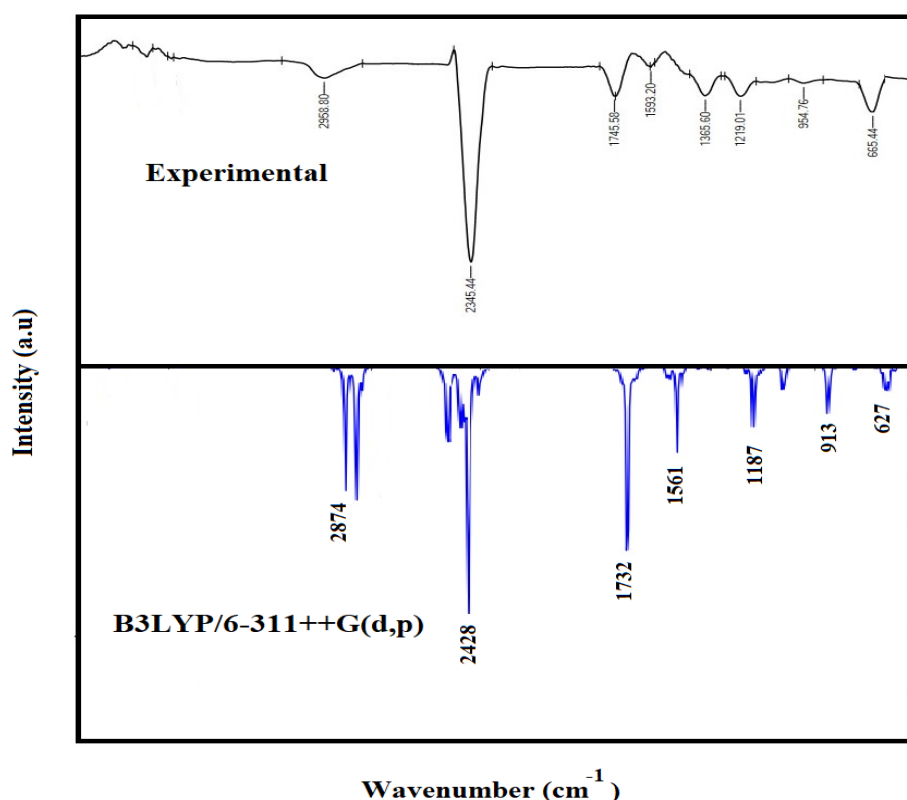
Figure.3 FTIR spectrum of 2APDM crystal

Table .1FT-IR and simulated band assignment of 2APDM complex

Observed wavenumbers (cm^{-1})		Assignment
FT-IR	**B3LYP**	
2958 and 2345	2874 and 2428	CH stretching vibration
1745	1732	NH asymmetric stretching vibration
1593	1561	NO$_2$ asymmetric stretching vibration
1365	-	CH deformation
1219	1187	CO stretching vibration
954	913	CC stretching vibration
665	630	CBr stretching vibration

3.3 Hirshfeld surface analysis

The Hirshfeld surface analysis is an essential tool for understanding the interactions [11]. The intermolecular interactions were analyzed by crystal explorer 3.1 [12], which produce Hirshfeld surface (Figure 4) of the compound. The de and di surfaces indicate the hydrogen donor and acceptor interactions through dark red spots. The d$_{norm}$ red spot indicates the strong interactions on the molecule, weak interactions over the blue region, and white regions indicate no interactions. The fingerprint plots of atom-atom interactions (Figure 5) indicated that the intermolecular and intramolecular interactions were observed between Br…C, Br…H, C…H, H…H and H…N. the stability of the material was emphasized by strong interactions between aminopyridine and the dibromomethane ion.
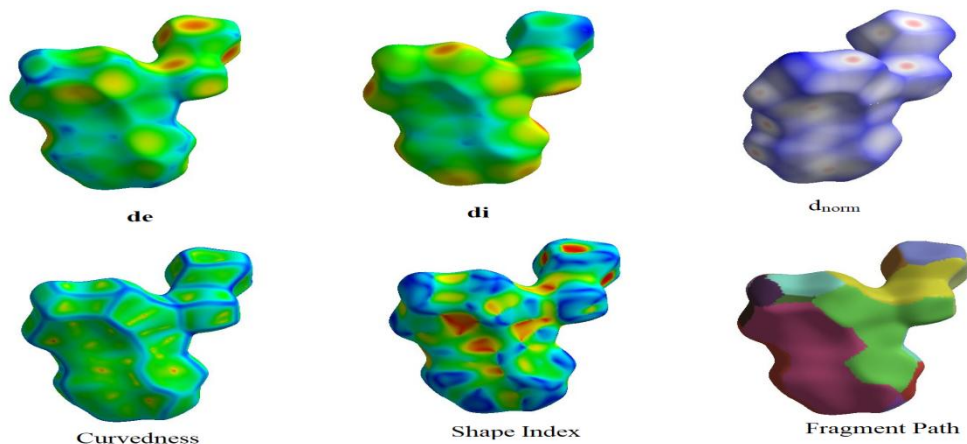
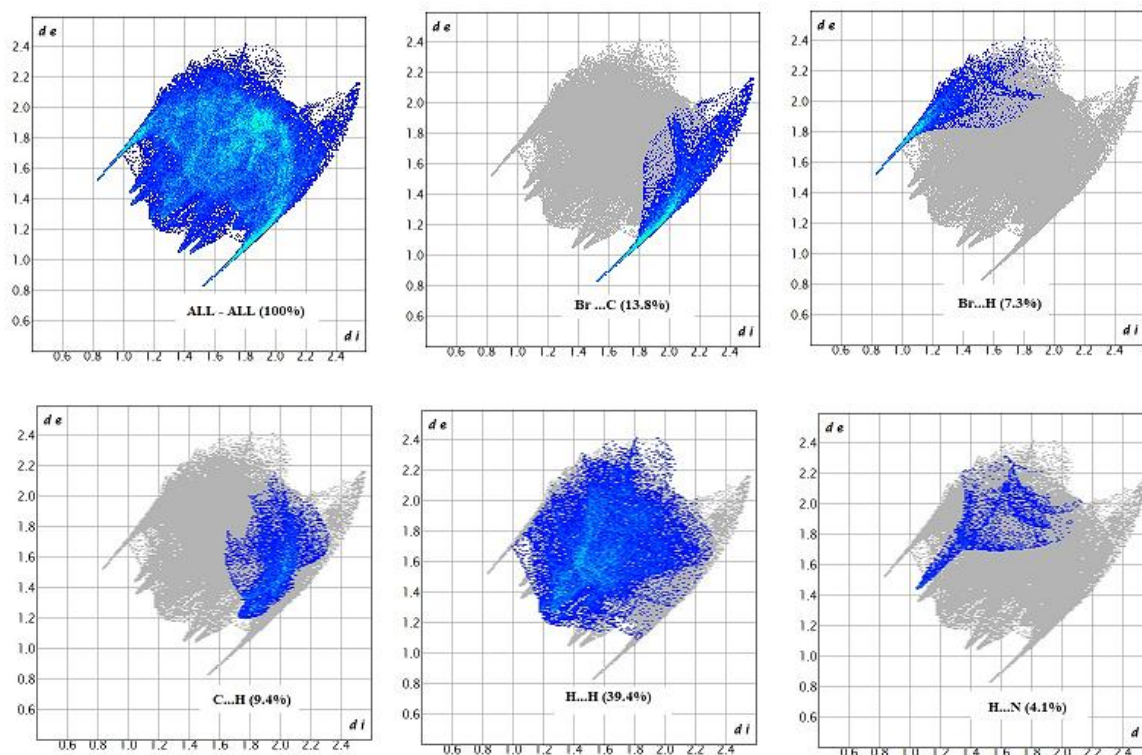**Figure 4.Hirshfeld surface analysis of 2APDM.**

Figure 5.Finger plots of 2APDM.

4. COMPUTATIONAL DETAILS

The entire calculations was performed at DFT/B3LYP levels with the standard basis set 6-311++G (d,P) on personal computer using GAUSSIAN 09W [13] program package, invoking gradient geometry

optimization [14]. Subsequently, the vibrations in association with the molecule were derived along with their IR intensity. The HOMO−LUMO (highest occupied molecular orbital and lowest unoccupied molecular orbital) analysis has been carried out to explain the inter molecular interactions within the molecule. The natural bonding orbital's (NBO) calculations [15] were performed using program as implemented in GAUSSIAN 09W package at DFT level.

4.1 Electronic Absorption Spectra

The electronic transitions of 2APDM, TD-SCF/B3LYP/6-311++G (d,p) calculations were used. The spectra were recorded in gas and other solvents (Acetone and Water) which are represented in Figure 6 in comparison with the experimental one. The maximum absorption in gas took a position at 380.91 nm, but the absorption peaks in all other solvents exhibited small variations than in gas possibly due to the solvent effect. The UV absorption was found to be much stronger than that in the visible region. It was found that the calculated line shape and relative strengths of peaks are in good agreement with those of the experimental results [16]. Table 2 shows the calculated and experimental wavelengths from absorption (λ_{max}), % contribution from each transition, transition energies (E_t) and oscillator strength (f) computed at the B3LYP/6-311++G (d,p) level for 2APDM in gas and different solvents (Acetone and Water).
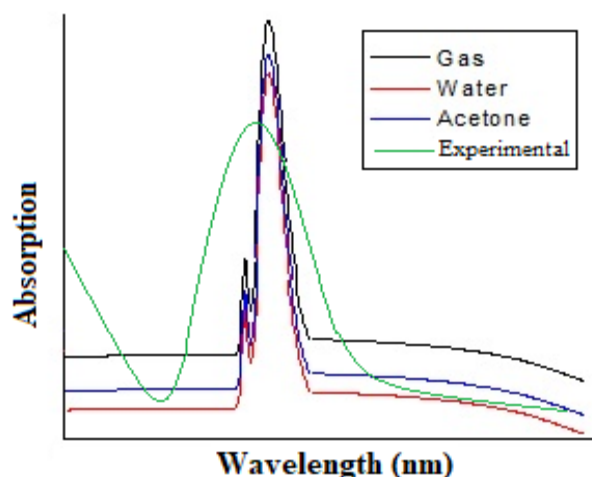

Figure.6 Experimental and Theoretical UV absorbance spectrum (Recorded by B3LYP/6-311++G (d,p) in different solvents) of 2APDM.

Table 2. Experimental and calculated electronic transition parameters of 2APDM by a B3LYP/6-311++G (d,p) method in gas and other solvents.

Solvent	Spectrum	Electronic Transition	E_t	λ_{max}		f	ε (%)
				Experimental	Calculated		
Gas	UV	Excited state I (H-4)-L (H-3)-L (H-2)-L	3.1880		380.91	0.3472	321518
		Excited state II (H-	3.4543		313.95	0.0033	19993

Solvent	Method	Transition	E_t		λ_{max}	f	$\mathcal{E}$
		1)-L H-L					
		Excited state III (H-1)-L H-L	3.5649		312.47	0.0007	90556
Acetone	UV	Excited state I (H-4)-L (H-3)-L (H-2)-L	3.8278		371.93	0.0005	303513
		Excited state II (H-1)-L H-L	4.1748		296.98	0.0007	29993
		Excited state III (H-1)-L H-L	4.1249		290.50	0.0016	91447
Water	UV	Excited state I (H-	3.8331	358	370.61	0.0005	312011
		4)-L (H-3)-L (H-2)-L					3
		Excited state II (H-1)-L H-L	4.2178		293.59	0.0007	34992
		Excited state III (H-1)-L H-L	4.3132		287.54	0.0017	89553

*H-HOMO, L-LUMO

E_t – Transition energy (eV)

λ_{max} – Electronic absorption wavelength (nm)

f – Oscillator strength

$\mathcal{E}$ - Contribution (%)

4.2 Frontier Molecular Orbital (FMO) Analysis

The orbital energy level analysis for 2APDM on the DFT/B3LYP/6-311++G(d,p) level indicates E_{HOMO} (highest occupied molecular orbital) and E_{LUMO} (lowest unoccupied molecular orbital) values of -3.9119eVand -3.5424eV, respectively. The significance of the HOMO-LUMO energy separation should implythe reactivity pattern of the molecule. The charge densities of the HOMO and LUMO are proved in Figure 7.The DFT level calculated energy gap is 0.3695eV.
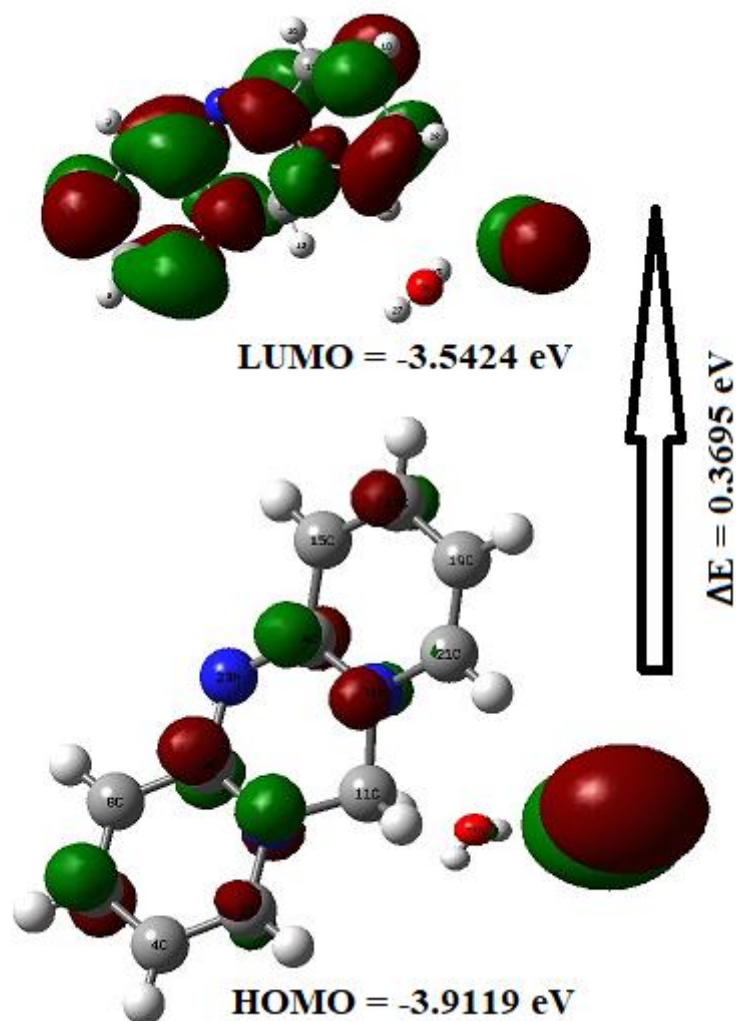
LUMO = -3.5424 eV

ΔE = 0.3695 eV

HOMO = -3.9119 eV

Figure 7. TheHOMOandLUMOorbitalfor 2APDM

4.3Determination of dipole moment (μ), Polarizability (α) and First order hyperpolarizability (β)

The calculation of static dipole moment (μ), Polarizability (α) and First order hyperpolarizability (β) for the better understanding of the electronic structure of the material and their NLO behavior can be well depicted through the Quantum Chemical approach [17] from which the correlation between the structure and the NLO activity can be easily described. The NLO properties are very much influenced by the values of dipole moment, electron mobility, polarizability and hyperpolarizability [18-20]. The increase in the values of polarizability and hyperpolarizabilities results with increasing NLO properties in a material. The NLO properties of a 2APDM molecule such as molecular dipole moment (μ), mean polarizabilityb(α), anisotropy of the polarizability (Δα) and first order molecular hyperpolarizabilities (β) have been investigated using DFT method with B3LYP level with 6-311++G(d,p) basic set using the below equations.

$\mu_{tot} = (\mu_x + \mu_y + \mu_z)^{\frac{1}{2}}$

$\alpha_{tot} = \frac{1}{3}(\alpha_{xx} + \alpha_{yy} + \alpha_{zz})$

$\Delta\alpha = \frac{1}{\sqrt{2}}[(\alpha_{xx}-\alpha_{yy})^2 + (\alpha_{yy}-\alpha_{zz})^2 + (\alpha_{zz}-\alpha_{xx})^2 + 6\alpha_{xz}^2 + 6\alpha_{xy}^2 + 6\alpha_{yz}^2]^{\frac{1}{2}}$

$\beta_{tot} = [(\beta_{xxx} + \beta_{xyy} + \beta_{xzz})^2 + (\beta_{yyy} + \beta_{yzz} + \beta_{yxx})^2 + (\beta_{zzz} + \beta_{zxx} + \beta_{zyy})^2]^{\frac{1}{2}}$

The first order molecular hyperpolarizabilioty (β) is denoted by 3 x 3 x 3 matrix, which is a third rank tensor. On account of Kleinman symmetry, the 27 elements of the 3D matrix will be reduced to 10 components. The values of polarizability and hyperpolarizability tensors are acquired by Gaussian frequency job output file which are given in table 3. The calculated values of along with their tensor components are also listed in the Table 3. The estimated values polarizability and hyperpolarizabilities are converted into electrostatic units (e.s.u) since the values were reported in atomic units (a.u). the values of polarizability are converted using 1 a.u = 0.1482 x 10^{-24}esu, similarly for β values are converted using 1 a.u = 8.6393 x 10^{-33}esu [21, 22]. For the present compound, the estimated values of μ, α, Δα and β are found 9.7072 D, 15.6601 x10^{-23}esu, 48.3617 a.u.and 0.464286x10^{-30}esu to be respectively.

Dipole moment (Debye)		Hyperpolarizability (a.u)	
Parameter	B3LYP/ 6-311++G (d,p)	Parameter	B3LYP/ 6-311++G (d,p)
μ_x	-9.6795	β_{xxx}	-8.3171
μ_y	0.2228	β_{yyy}	10.4069
μ_z	0.6978	β_{zzz}	0.2667
μ	9.7072	β_{xyy}	6.5845
Polarizability ($\mathring{A}^3$)		β_{xxy}	-48.5784
α_{xx}	-128.3487	β_{xxz}	-1.1722
α_{xy}	1.3352	β_{xzz}	28.1260
α_{xz}	6.0038	β_{yzz}	-2.4476
α_{yy}	-75.6969	β_{yyz}	-22.3665
α_{yz}	2.0951	β_{xyz}	-6.6623
α_{zz}	-112.9622	β_{Tot}	0.46428x10^{-30}esu

α_{Tot}	15.6601×10^{-23} esu
$\Delta\alpha$	48.3617 a.u

Table 3. The electric dipole moment (μ), polarizability (α_{Tot}) and hyper polarizability (β_{Tot}) at APCC at B3LYP6-311++G(d,p) method.

.4 NBO Analysis

The charge transfer interactions connecting the bonds are determined using natural bond orbital analysis. The molecule's NBO was calculated at the B3LYP/6-311++G (d, p) level. The estimation of the off-diagonal NBO Fock matrix elements F(i,j) is provided by this energy interaction which is acquired using the second-order perturbation method [23, 24]. From NBO analysis, the one-centre lone pairs and two-centre bonds illustrate the chemical bonding for a stable molecular species, to the respective single Lewis structure. In addition to the valence anti-bonds (BD*), the non-Lewis set comprises unoccupied valence nonbonding (LP*) and extra-valence-shell Rydberg (RY*) orbitals. The deficiency of the Lewis-type NBOs (bonds and lone pairs) in indicating the density matrix may be quantified with the occupancy of those NBOs. The energy of the delocalization, *Eij* is calculated as

$$E(2)=\Delta E_{ij} = q_i F(i,j)^2 / (\varepsilon j - \varepsilon i)$$
(1)

Wherein(1) is the energy of hyper conjugative interactions. Q_i is the occupancy of the donating (Lewis type) orbital, εi and εj are the energies of the donating and accepting orbitals, and F_{ij} is the off-diagonal element of the Fock matrix inside the NBO basis **.**NBO analysis was performed on the2APDM molecule at the B3LYP/6-311++G(d,p) level to explain intramolecular hybridization and electron density delocalization within the molecule.

In computational chemistry, the natural bond orbital (NBO) analysis is used to calculate bonds, donor-acceptor interactions, bond order, and electron density distribution among atoms [25]. Table 4 shows the results of the analysis. The intramolecular hyper conjugative interactions are formed by overlapping the orbitals between bonding (C-C) and (C-N) and anti-bonding (C-C)and (C-N) orbital which outcomes in intramolecula charge transfer (ICT) stabilizing the molecular system which leads to increase in electron density. Interaction between the antibond (C14-N24), (C10-N23) to antibonding (C10-N23), (C6-C8) is seen to give the strongest stabilization (102.6 KJmol^{-1}, 75.92KJmol^{-1}) similarly interaction between the nitrogen lone pair and the antibond (C10-N23), (C2-C4) is seen to give the strong stabilization energy (56.93 and 35.08KJmol^{-1}).

Table 4.Second-order perturbation theory analysis of Fock matrix in NBO basis of 2APDM

Donor(i)	E D (i) (e)	Acceptor(j)	ED(j)(e)	E(2)[a] (kcal/mol)	E(j)- E(i)[b] (a.u.)	F(i,j)[c] (a.u.)
π(C2 - C4)	1.77101	π*(C 6– C8)	0.20833	18.22	0.32	0.069
π(C6 – C8)	1.71658	π*(C10 – N23)	0.51922	26.52	0.27	0.080
π(C10 – N23)	1.75320	π*(C14– N24)	0.64031	45.28	0.26	0.107
π(C15 - C17)	1.71157	π*(C14 – N24)	0.64031	31.87	0.22	0.082
π(C19-C21)	1.73779	π*(C15– C17)	0.20532	18.89	0.32	0.070
n(1) N25	1.55738	π*(C 2 – C4)	0.21931	35.08	0.31	0.098
n(1) N25	1.55738	π*(C 10 – N23)	0.51922	56.93	0.29	0.116
π*(C10 – N23)	0.51922	π*(C 6 – C8)	0.20833	75.92	0.04	0.082
π*(C14 – N24)	0.64031	π*(C 10 – N23)	0.51922	102.06	0.04	0.077
π*(C14 – N24)	0.64031	π*(C 15 – C17)	0.20532	42.76	0.09	0.087

ED(e) is the electron density of donor and acceptor of NBO orbitals.

a. E(2) means the energy of hyperconjugative interactions.

b. Energy difference between donor and acceptor i and j NBO orbitals.

c. F(i,j) is the Fock matrix element between i and j NBO orbitals.

4.5 Molecular electrostatic potential (MEP)

The MEP map for the 2APDM molecule was carried out using B3LYP/6-311++G(d,p) basis set. The three dimensional MEP map of the 2APDM compound encompassing different color codes between deepest red and deepest blue, ranging from -0.106 to 0.106 eV is shown in the Figure 7. Red, blue and green are the three important colors which decide the value of the electrostatic potential. The value of the potential expands in the sequence red < orange < yellow < green < blue. The blue regions on the surface signifies the positive value of the potential which are electron deficient areas, the red regions indicates the negative value of the map which are highly electron rich areas, whereas the zero potential of the map will be denoted by the green color [28,29]. The yellow and light blue regions on the surfaces are slightly electron rich and slightly electron different areas. As the negatively charged surfaces (high electron density) such as red and yellow color regions are targeted to electrophiles or protons and hence are meant for electrophilic attack whereas the positively charged surfaces (low electron density) such as blue and light blue regions are associated with nucleophilic attack. The blue and red region on the surface signifies the strongest attraction and repulsion respectively [30]. It is clear from the figure, while area having the negative potential is over the electronegative

atom (oxygen atom), the regions having the positive potential are over the hydrogen atoms.
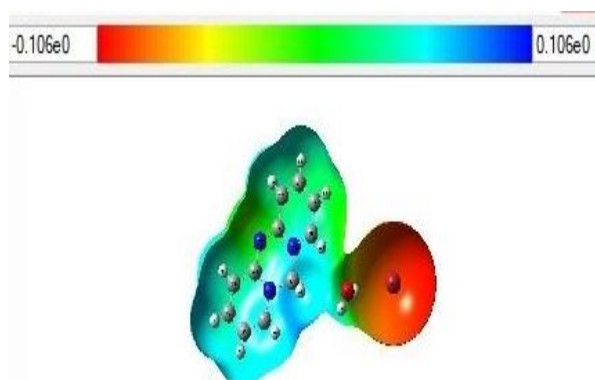

Figure 7.Calculated 3D molecular electrostatic potential contour map of 2APDM.

4.6Mulliken population analysis (MPA) and Natural population analysis (NPA)

Mulliken population analysis (MPA) and Natural population analysis (NPA) by the usage of B3LYP/6-311++G(d,p) method helps to yield the following charge distributions on various atoms (Br, C, N, H, and O) in Table 5. The Mulliken atomic charges and Natural atomic charges study of CPM (cluster partitioning method) using the B3LYP/6-311++G(d,p) method is depicted in Figure 8.The appearance of hydrogen or oxygen tends the carbon atom to be more electron-deficient. Positive charges are found in all hydrogen atoms. The 22 Hatom has a more positive charge of 0.371544 as compared to other carbon atoms.

Table 5.Mulliken Atomic Charge and Natural Atomic Charge of 2APDM

Atoms	B3LYP	
	MPA	NPA
1 Br	-0.636081	-0.84696
2 C	0.188764	0.10687
3 H	0.046542	0.17605
4 C	-0.334634	-0.19767

| 5 H	0.216742	0.18879
6 C	-0.299051	-0.09536
7 H	0.204721	0.17850
8 C	0.140814	-0.16693
9 H	0.215309	0.19651
10 C	-0.225382	0.43171
11 C	-0.134380	0.08249
12 H	-0.139017	0.20197
13 H	0.347183	0.18886
14 C	0.333114	0.43699
15 C	0.185007	-0.17920
16 H	0.215185	0.19506
17 C	-0.309074	-0.07576
18 H	0.204625	0.17825
19 C	-0.413964	-0.18868
20 H	0.199109	0.19567
21 C	0.047312	0.12871
22 H	0.371544	0.20760
23 N	-0.080641	-0.56547
24 N	0.209322	-0.38520
25 H	0.174598	-0.38726
26 H	0.268071	0.46813
27 H	0.268071	0.41823
28 O	-0.515435	-0.89190
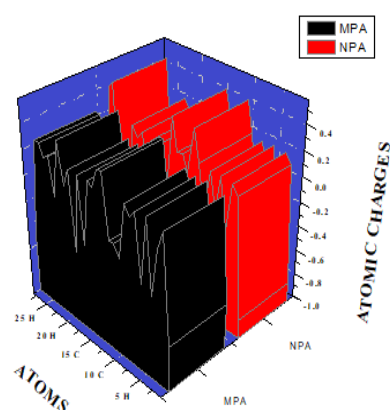
Figure 8.Mulliken population analysis and Natural population analysis

4.7 Global Chemical Reactivity Descriptors (GCRD)

The energy values computed using DFT method was further utilized to investigate the structural stability and global chemical reactivity of the molecule [31]. As stated by FMO theory, the energy values of HOMO and LUMO are very much analogous to the ionization potential (I) and electron affinity (A) respectively which can be expressed as,

Ionization potential (I) = $-E_{HOMO}$ = 3.9119eV

Electron affinity (A) = $-E_{LUMO}$ = 3.5424eV

Both these ionization potential and electron affinity derived using energy values give rise to different global chemical reactivity descriptors and their by helps in elucidating the molecular or atomic properties and calculating some chemical quantities [32]. The other parameters of GCRDs of the compound including Electronegativity (χ), Chemical hardness (η), global softness (σ), electrophilicity (ω), and chemical potential (μ), etc., which are defined on the basis of Koopman's equation [33] [computed at Gas [DFT- B3LYP/ 6-311++G(d,p)]] by the following relations [34].

The Electronegativity of the molecule estimated as, $(\chi) = \left(\frac{I+A}{2}\right)$

The absolute hardness of the molecule calculated as, $(\eta) = \frac{I-A}{2}$

The global softness (inverse of hardness) of the molecule evaluated as, $\sigma = \frac{I}{\eta}$

The chemical potential of the molecule approximated as, $\mu = -\left(\frac{I+A}{2}\right)$ or $-(\chi)$

The value of electrophilicity index determined as, $\omega = \frac{\mu^2}{2\eta}$

The global chemical reactivity descriptors calculated using HOMO – LUMO energy values reveals that the molecule holds good kinetic stability [35] with the hardness value of 0.1847eV. The value (37.60eV) exhibited by electrophilicity index (ω) endorse the electrophilic behavior of the molecule. The negative value of the chemical potential indicates the stability of the molecule. The estimated GCRDs in the present work confirm the excellent chemical strength and stability of the molecule and hence favor the suitability of the material for optoelectronic applications. The calculated values energy gaps, E_{HOMO}-E_{LUMO} together with various GCRDs are listed in the Table 6.

Table 6.Calculated electronic properties and quantum parameters of 2APDM at DFT/ B3LYP / 6-311++G (d,p) level.

Parameters	Gas [DFT/ B3LYP /6-311++G (d,p] (eV)
E_{HOMO}	-3.9119
E_{LUMO}	-3.5424
E_{gap}(eV)	0.3695
Ionization potential (I)	3.9119
Electron affinity (A)	3.5424
Electronegativity (χ)	3.7271
Chemical hardness (η)	0.1847
Chemical potential (μ)	-3.7271
Global softness (σ)	21.17
Electrophilicity (ω)	37.60
Dipole moment (Debye)	9.7072

4.8 Molecular Docking

PASS (prediction of activity spectra) is an online tool which predicts different types of activities based on the structure of a compound [36]. Molecular docking is an efficient tool to get an insight into ligand-receptor interactions and screen molecules for the binding affinities of a particular receptor. All molecular docking calculations were performed on AutoDock-tool software [37]. The 3D structure of oxidoreductase protein 2FYU [38]was obtained from protein data bank (PDB ID: 4Z9Q) [39]. 2APDM structure

was created by using "Chemdraw". The AutoDock tools graphical user interface was used to calculate Geisteger charges, add polar hydrogen and partial charges using Kollman united charges. The active site of the enzyme was

definedtoincluderesiduesoftheactivesitewithint hegridsizeof62Åx68Åx64 Å. The most popular algorithm, Lamarckian Genetic Algorithm (LGA) available in AutoDock was employed for docking. Docking protocol was tested by docking the co-crystallized inhibitor onto the enzyme catalytic site which showed perfect energy .within the cocrystallized ligand with RMSD well within the allowed range of 2 Å. The present study helps us to understand the interaction between the title compound and receptor oxidoreductase protein 2FYUand also explore their binding mode (Figure 9,10). The calculated the binding energy value is 1.28 Kcal/mol.Estimated inhibition constant 105.13mM and RMSD value is 71.80Å. Our docking results indicated that the said compound bound in the pocket includes the residues construct the active pocket of oxidoreductase protein.

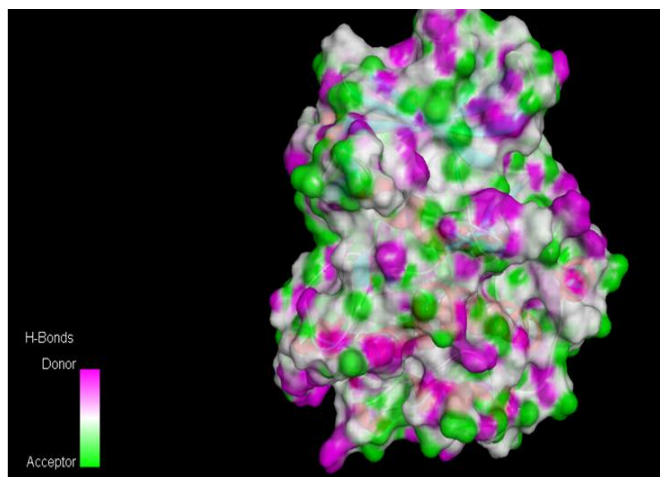**Fig 9 Prepared Strucure of the chain A protein 2FYU taken from pymol software**

Figure 10. Docked acceptor-donor surface view taken from Discovery studio software

5. Conclusion

In conclusion, the present study deals with the crystal growth, physical characterization, and in-depth molecular orbital energy analysis of the 2APDM single crystal. From the characterization, the single-crystal X-ray diffraction analysis indicates the monoclinic system of 2APDM. Also, the powder XRD studies indicated the identification of crystalline planes where the peaks are properly indexed. The FTIR spectral analysis shows the appropriate functional groups for the 2APDM compound. Further, with the 2APDM crystals, using DFT theoretical calculation we performed the optimized geometrical parameters based on B3LYP levels of theory with the standard basis set 6-311++G (d,p). We observed that the stability has enhanced due to the HOMO-LUMO energy gap of the 2APDM molecule. Similarly, the natural bond orbital analyses used for the investigation of stabilization energy of various inter and intramolecular interaction within the systems and the net charge distribution of the 2APDM compound was computed by the Mulliken atomic charge and Natural atomic charge analysis.The calculated GCRD parameters such as I, A, χ,

η, σ, ω, μ shows that the material possesses good chemical strength and kinetic stability and the calculated values favors the good candidate suitable for optical applications. The binding energy for 2APDM is 1.28 kcal/mol, and docked inhibitors interacted with the ligand within the 2FYU binding site, according to the docking output.

Conflict of interest:

The authors declare no conflict of interest with this work.

Acknowledgment

References

[1] H.S. Nalwa, Organometallic materials for non linear optics, Appl. Organomet. Chem.5 (1991)349-377

[2] B. K. Periyasamy, R.S. Jebas, B. Hailampillai, Mater, Lett. 61 (2007) 1489

[3] R.W. Munn, C.W. Ironside, Principles and applications of Nonlinear Optical Materials, Crc Press,   Inc, Usa, 1994.

[4] l.R. Kaino, B. Cai, K. Takayama, Adv.Funct. Mater.12 (2002) 599.

[5] J.R. Bardon R. Hierle, A. Periguard, J. Zyss, D.J. Williams, Nonlinear optical properties of organic molecules and polymeric materials, Acs

Ser. 223 (1993) American chemical society, Washington Dc.

[6] Chenthamarai, S., Jayaraman, D., Ushasree, P.M., Meera, K., Subramaniyan, C.,

Ramasamy, P., Mater Chem. Phys. 54, 179-183 (2000).

[7] L. R. Dalton, P. A. Sullivan, B.C. Olbrich, D.H. Bale, J. Takayesu, S. Hammond, H. Rommel, B.H. Robinson, Tutorials in Complex Photonics Media , Spie, Bellingham, Wa, 2007.

[8] Kechen Wu.; Caiping Liu.; Caiping Liu.; ChaoyongMang.; Opt. Mater, 2007, 29, 129.

[9] D. S. Chemla, J.Zyss, Non Linear Optical properties of Organic Molecules and Crystals, Academic Press, New York, 1987.

[10] Xian-WuJiang, Heng-qiang Zhang, Zhuo-Dong Sun and Young-KuiShan ., IUCrData (2016). 1, x160180.

[11] McKinnon JJ, Jayatilaka D, Spaceman MA (2007) Towards Quantitative analysis of intermolecular interactions with Hirshfeld surfaces. ChemCommun: 3814-3816.

[12] Turner MJ, McKinnon JJ, Wolff SK, Grimwood DJ, Spackman PR, Jayatilaka D, Spaceman MA (2017), Crystal Explorer, p 17.

[13] Frisch, M.J.(2009). GAUSSIAN 09, Revision **A. 9**, Gaussian, INC, Pittsburgh.

[14] Schlegel,H.B.J. Comput. Chem. **3**, (1982).pp.214−218.

[15] Glendening,E.D. Reed,A.E.Carpenter,J.E.&Weinhold, F.(1998). NBO Version 3.1.TCI.

[16] Xu J.; Wang L.; Liang G.; Bai Z.; Wang L.; Xu W.; Shen X.;Spectrochim. Acta A, 2011,78, 287-293.

[17] K. Govindarasu, E. Kavitha, Molecular structure, Vibrational spectra, NBO, UV and first order Hyperpolarizability, analysis of 4-Chloro-DL-phenylalanine by Density Functional Theory, SpectrochimicaActa Part A: Molecular and Biomolecular Spectroscopy, 133,799-810, 10 (2014).

[18] P. Muthuraja, T. JoselinBeaula, T. Shanmugavadivu, V. BenaJothy, M.

Dhandapani, Hydrogen bonded R2 (8) graph set in inducing charge transfer mechanism in guanidium-3,5-dinitrobenzoate: A combined experimental, theoretical and Hirshfeld surface study, J. Mol. Structure 1137, 649-662, 5 (2017).

[19] BasakKosar, CigdemAlbayrak, Spectroscopic investigations and quantum chemical computational study of (E)-4-methoxy-2-[(p-tolylimino)methyl]phenol, SpectrochimicaActa Part A: 78, 160-167, (2011).

[20] V. Balachandran, K. Parimala, Molecular structures, FT-IR and FT-Raman spectra, NBO analysis, NLO properties, reactive sites and quantum chemical calculations of keto-enaltautomerism (2-amino-4-pyrimidinol and 2-amino-pyrimidine-4(1H)-one, SpectrochimicaActa Part A: Molecular and Biomolecular Spectroscopy, 102, 30-51, (2013).

[21] M. Raja, R. Raj Muhamed, S. Muthu, M. Suresh, Synthesis, spectroscopic (FTY-IR, FT-Raman, NMR, UV-Visible), NLO, NBO, HOMO-LUMO, Fukui function and molecular docking study of (E)-1-(5-bromo-2-hydroxybenzylidene)bsemicarbazide, J. Mol. Stru. 1141, 284-298, 5 (2017).

[22] Shivaraj R. Maidur, ParutagoudaShankaragoudaPatil, Z-scan studies of third-order nonlinear optical limiting properties of chalcones doped Poly9methylmethaacrylate) thin films for visible laser production, Optical Materials 84, 28-37, (2018).

[23] Na, L.J.; Rang, C.Z.; Fang, Y.S.; J. Zhejiang Univ. Science, 2005, 6B, 584–589.

[24] Dannenberg, J.J.; Chem. Rev, 1999, 99, 1225-1241.

[25] Raja, M.; Muhamed, R.R.; Muthu, S.; Suresh, M.; J. Mol. Structure, 2017, 1141, 284-298.

[26] Kaur, M.; Mary, Y.S.; Varghese, Y.S.; Panicker, C.Y.; Yathirajan, H.S.; Siddegowda, M.S.; Van Alsenoy, C.; Spectrochim. Acta A, 2012, 98, 91–99.

[27] Rastogi, V.K.; AlcoleaPalafox, M.; Tamoou, R.P.; Mittal, L.; Spectrochim. Acta A, 2002, 58, 1987–2004.

[28] HenaKhanum, Ashraf Mashrai, NaziahSiddiqui, Musheer Ahmed, Mohammed Jane Alam, Shabbir Ahmed, Shamsuzzaman, Structural elucidation, density functional calculations and contribution of intermolecular interactions in cholest-4-en-3-one crystals: Insights from X-ray and Hirshfeld surface analysis, J. Mol. Structure, 1084, 274-283, (2015).

[29] M. Raja, R. Raj Muhamed, S. Muthu, M. Suresh, Synthesis, spectroscopic (FTY-IR, FT-Raman, NMR, UV-Visible), NLO, NBO, HOMO-LUMO, Fukui function and molecular docking study of (E)-1-(5-bromo-2-hydroxybenzylidene)bsemicarbazide, J. Mol. Stru. 1141, 284-298, 5 (2017).

[30] S. GhanbariNiyaki, M. Montazerozohori, A. Masoudiasl, J. M. White, New five coordinated supramolecular structured cadmium complex as precursor for cdo nanoparticles: Synthesis, crystal structure, theoretical and 3D Hirshfeld surface analysis, J. Mol. Structure, 1113, 201-211, 5 (2017).

[31] Shivaraj R. Maidur, ParutagoudaShankaragoudaPatil, AnushaEkbote, TzeShyang Chia, ChingKhengQuah, Molecular structure, second- and third-order nonlinear optical properties and DFT studies of a novel non-centrosymmetricchalcone derivative: (2E)-3-(4-flurophenyl)-1-{[(1E)-(4-fluorophenyl)methelene]amino}phenyl)prop-2-en-1-one, SpectrochimicaActa Part A: Molecular and Biomolecular Spectroscopy, 184, 342-354, (2017).

[32] Rajesh Kumar, Amit Kumar, VipinDeval, Archana Gupta, PoonamTandon, P. S. Patil, PrathmeshDeshmukh, DeepikaChaturvedi, J. G. Watve, Molecular structure, spectroscopic (FT-IR, FT Raman, UV, NMR and THz) investigation and hyperpolarizability studies of 3-(2-Chloro-6-fluorophenyl)-1-(2-thienyl) prop-2-en-1-one, 1129, 292-304, (2017).

[33] P. Dhamodharan, K. Sathya, M. Dhandapani, Physico-chemical characterization, density functional theory (DFT) studies and Hirshfeld surface analysis of a new organic optical material: 1H-benzo[d]imidazol-3-ium-2,4,6-trinitrobenzene-1,3bis(olate), J. Mol. Structire 1146, 782-792, 15 (2017).

[34] Karthik Kumara, A. Dileep Kumar, S. Naveen, K. Ajay Kumar, N. K. Lokanath, Synthesis, spectral characterization and X-ray crystal structure studies of 3-(benzo[d][1,3]dioxol-5-yl)-5-(3-methylthiophen-2-yl)-4,5-dihydro-1H-pyrazole-1-carboxamide: Hirshfeld surface, DFT and thermal analysis, J. Mol. Structure, 1161, 285-298, (2018).

[35] Shivaraj, R. Maidur, Jitendra R. Jahagirdar, ParutagoudaShankaragoudaPatil, TzeShyang Chia, CjhingKhengQuah, Structural characterizations, Hirshfeld surface analyses, and third order nonlinear optical properties of two novel chalcone derivatives, Optical Materials, 75, 580-594, (2018).

[36] http://www.passonline.org

[37] http://www.rcsb.org

[38] O. Trott, A.J. Olson, J. Comput. Chem. 31 (2010) 455.

[39]Esser,L., Gong,X., Yang,S., Yu,L., Yu,C.A., Xia, (2006) ProcNatlAcadSci U S A **103**: 13045-13050